Structural Engineering and Mechanics, *Vol. 70, No. 2 (2019) 143-152*
DOI: https://doi.org/10.12989/sem.2019.70.2.143

Spatially variable effects on seismic response of the cable-stayed bridges considering local soil site conditions

Zeliha Tonyali*[1], Sevket Ates[2] and Suleyman Adanur[2]

[1]*Department of Civil Engineering, Recep Tayyip Erdogan University, 53100, Rize, Turkey*
[2]*Department of Civil Engineering, Karadeniz Technical University, 61080, Trabzon, Turkey*

(Received August 6, 2018, Revised February 14, 2019, Accepted February 20, 2019)

Abstract. In this study, stochastic responses of a cable-stayed bridge subjected to the spatially varying earthquake ground motion are investigated for variable local soil cases and wave velocities. Quincy Bay-view cable-stayed bridge built on the Mississippi River in Illinois, USA selected as a numerical example. The bridge is composed of two H-shaped concrete towers, double plane fan type cables and a composite concrete-steel girder deck. The spatial variability of the ground motion is considered with the coherency function, which is represented by the components of incoherence, wave-passage and site-response effects. The incoherence effect is investigated by considering Harichandran and Vanmarcke model, the site-response effect is outlined by using hard, medium and soft soil types, and the wave-passage effect is taken into account by using 1000, 600 and 200 m/s wave velocities for the hard, medium and soft soils, respectively. Mean of maximum response values obtained from the analyses are compared with those of the specific cases of the ground motion model. It is concluded that the obtained results from the bridge model increase as the differences between local soil conditions cases of the bridge supports change from firm to soft. Moreover, the variation of the wave velocity has important effects on the responses of the deck and towers as compared with those of the travelling constant wave velocity case. In addition, the variability of the ground motions should be considered in the analysis of long span cable-stayed bridges to obtain more accurate results in calculating the bridge responses.

Keywords: wave-passage effect; incoherence effect; site-response effect; stochastic response; cable-stayed bridge; spatially varying earthquake ground motion

1. Introduction

In order to determine the effects of earthquake ground motions on the dynamic response of small structures, such as buildings, a well-established assumption is that the ground motions over the entire foundation area of the structure are fundamentally the same. In other words, the earthquake ground motions between bridge supports are considered to be uniform. However, for long span bridges, such as cable-stayed bridges, this assumption may be unrealistic for the real ground motion due to owing to the earth structure complexity, the difference between local soil conditions at structural support points and the seismic wave propagation changes its characteristics. Consequently, earthquake motions will be subjected to significant variations at support points of long-span structural systems. Current several researches signify that the seismic response of large span structures may become larger when the spatial effects are considered (Allam and Datta 1999, Ates *et al.* 2005, Soyluk and Dumanoglu 2004, Thomas and Marc 1998, Wang *et al.* 2009, Zhang *et al.* 2009). All these studies underline the importance of the spatially varying ground motion effect. Therefore, multi-point earthquake excitations should be considered in these types of long span bridges.

Nazmy and Abdel Ghaffar (1987, 1990, 1992) performed linear and non-linear earthquake response analysis of cable-stayed bridges subjected to as well as multiple support uniform seismic excitations. In these studies, it is indicated that the multiple-support seismic excitations should be considered in the earthquake-response analysis of such long span and complex structures. Betti *et al.* (1993) studied the dynamic effects of soil–structure interaction on the response of cable-supported bridges subjected to multiple-support seismic excitation and outlined the importance of multiple-support seismic excitation and soil-structure interaction effects. Garevski *et al.* (1988) and Soyluk and Dumanoglu (2000) carried out dynamic analyses of cable-stayed bridges for delayed support excitations and concluded that any seismic analysis of even moderately long cable-stayed bridges requires the consideration of the velocity of ground motion. Soyluk and Yucel (2007) performed the random vibration analyses of two different steel arch bridge models for the spatial variation of the ground motion including the wave passage effect. Allam (2010) examined the influence of the wave passage effect on the response of an open-plane frame building with soil–structure interaction. The ground acceleration was modeled by a suitably filtered white-noise. The results were discussed with regard to the wave passage and soil-structure interaction effects. Kuyumcu and Ates (2012) determined the soil-structure-foundation effects on stochastic response analysis of cable-stayed bridges. Geng

*Corresponding author, Assistant Professor
E-mail: zeliha_tonyali@erdogan.edu.tr

ISSN: 1225-4568 (Print), 1598-6217 (Online)

et al. (2014) investigated dynamic characteristics of the longest multi-span cable-stayed bridge in the world by using the commercial software package ANSYS. Yan *et al.* (2014) presented an alternative seismic design strategy for cable stayed bridges with concrete pylons when subjected to strong ground motions. Zhang and Yu (2015) examined seismic response of the cable-stayed-suspension hybrid bridges under the horizontal and vertical seismic excitations by response spectrum analysis and time history analysis. They compared their seismic performance the cable-stayed bridge and suspension bridge with the same main span.

Bai *et al.* (2015) examined dynamic response of angled beams subjected to impact loads by using the stochastic finite element method. In this study, statistics of displacement and stress waves were analyzed and effects of bend angle and material stochasticity on wave propagation were studied. Kim and Kang (2016) investigated the change of structural characteristics of steel cable-stayed bridges after cable failure. Wang *et al.* (2016) studied the wave-passage effect of earthquake loadings on long-span structures. From the study, it was obtained that the reduction of the maximum earthquake loading is fluctuant, but has a general tendency to decrease with the increase in the apparent wave velocity and the structural natural period. Adanur *et al.* (2017) investigated stochastic effects of the suspension bridges subjected to spatially varying ground motions for variable local soil cases and wave velocities. Ates *et al.* (2018) examined the effects of multiple support excitations and soil–structure interaction on the dynamic characteristics of cable-stayed bridges founded on pile foundation groups.

This paper presents a study of the wave-passage effect on the stochastic response of cable-stayed bridge subjected to spatially varying ground motions including the local site response effects. The main purpose of this study is to investigate the importance of the wave-passage effect including local site-response effect. In this content, the stochastic behavior of the cable-stayed bridge subjected to spatially varying ground motion by considering with the coherency function, which is represented by the components of incoherence, wave-passage and site-response effects is investigated. The incoherence effect is examined by taking into account Harichandran and Vanmarcke (1986) model. The site-response effect is outlined by using firm, medium and soft soil types proposed by Der Kiureghian and Neuenhofer (1991) and the wave-passage effect is investigated by using 1000, 600 and 200 m/s wave velocities for the firm, medium and soft soils, respectively. Mean of maximum response values obtained from the spatially varying ground motions are compared with those of the specialised cases of the ground motion model. Relative contributions of the pseudo-static, dynamic and covariance components to the total response are also presented.

2. Formulation

2.1 Random vibration theory for spatially varying ground motion

In the random vibration theory, the variance of the i. total response component is stated as (Harichandran *et al.* 1996)

$$\sigma_{z_i}^2 = \sigma_{z_i}^{2qs} + \sigma_{z_i}^{2d} + 2\,\mathrm{Cov}\,(z_i^{qs}, z_i^{d}) \tag{1}$$

where, $\sigma_{z_i}^{2qs}$ and $\sigma_{z_i}^{2d}$ are the variances of pseudo-static and dynamic response components, respectively and $\mathrm{Cov}\,(z_i^{qs}, z_i^{d})$ is the covariance between the pseudo-static and dynamic components and can be written as

$$\sigma_{z_i}^{2qs} = \int_{-\infty}^{\infty} S_{z_i}^{qs}(\omega)\,d\omega = \sum_{l=1}^{r}\sum_{m=1}^{r} A_{il}A_{im} \int_{-\infty}^{\infty} \frac{1}{\omega^4} S_{\ddot{v}_{gl}\ddot{v}_{gm}}(\omega)\,d\omega \tag{2}$$

$$\sigma_{z_i}^{2d} = \sum_{j=1}^{n}\sum_{k=1}^{n}\sum_{l=1}^{r}\sum_{m=1}^{r} \psi_{ij}\,\psi_{ik}\,\Gamma_{lj}\,\Gamma_{mk} \int_{-\infty}^{\infty} H_j(-\omega)\,H_k(\omega)\,S_{\ddot{v}_{gl}\ddot{v}_{gm}}(\omega) \tag{3}$$

$$\begin{aligned}\mathrm{Cov}\,(z_i^{qs}, z_i^{d}) = &-\sum_{j=1}^{n}\sum_{l=1}^{r}\sum_{m=1}^{r} \psi_{ij}A_{il}\Gamma_{mj} \\ &\cdot \int_{-\infty}^{\infty} \frac{1}{\omega^2} H_j(\omega)\,S_{\ddot{v}_{gl}\ddot{v}_{gm}}(\omega)\,d\omega\end{aligned} \tag{4}$$

where ω is the circular frequency, r is the number of support degrees of freedom where the ground motion is applied, n is the number of the modes used in the analysis. A_{il} and A_{im} are the static displacement components due to unit support motions, $S_{\ddot{v}_{gl}\ddot{v}_{gm}}$ is the cross-power spectral density function of accelerations between supports (l and m), $H(\omega)$ is the frequency response function.

2.2 Spatially varying ground motion model

The cross-power spectral density function of the accelerations and at the support points l and m is stated as (Der Kiureghian 1996),

$$S_{\ddot{v}_{gl}\,\ddot{v}_{gm}}(\omega) = \gamma_{lm}(\omega)\sqrt{S_{\ddot{v}_{gl}\,\ddot{v}_{gl}}(\omega)\,S_{\ddot{v}_{gm}\,\ddot{v}_{gm}}(\omega)} \tag{5}$$

Spatial variability of the ground motion is indicated with the coherency function in frequency domain. For the coherency function, the following model proposed by Der Kiureghian (1996) is used

$$\begin{aligned}\gamma_{lm}(\omega) &= \left|\gamma_{lm}(\omega)\right|^{k}\,\gamma_{lm}(\omega)^{d}\,\gamma_{lm}(\omega)^{z} \\ &= \left|\gamma_{lm}(\omega)\right|^{k}\exp\left[\,i\left(\theta_{lm}(\omega)^{d} + \theta_{lm}(\omega)^{z}\right)\right]\end{aligned} \tag{6}$$

where $\gamma_{lm}(\omega)^{k}$, $\gamma_{lm}(\omega)^{d}$ and $\gamma_{lm}(\omega)^{z}$ indicate incoherence, wave-passage and site-response effects, respectively.

For the incoherence effect, resulting from reflections and refractions of seismic waves through the soil throughout their propagation, the widely used model proposed by Harichandran and Vanmarcke (1986) is considered. This model is based on the analysis of

recordings made by the SMART-1 seismograph array in Lotung, Taiwan and defined as,

$$\left|\gamma_{lm}(\omega)\right|^k = A\,e^{\left[-\frac{2d_{lm}}{\alpha\,\theta(\omega)}(1-A+\alpha A)\right]} + (1-A)\,e^{\left[-\frac{2d_{lm}}{\theta(\omega)}(1-A+\alpha A)\right]} \quad (7)$$

where

$$\theta(\omega) = k\left[1+\left(\frac{\omega}{2\pi f_0}\right)^b\right]^{-0.5} \quad (8)$$

where d_{lm} is the distance between support points l and m. A, a, k, f_0 and b are model parameters and in this study the values obtained by Harichandran *et al.* (1996) are used (A=0.636, a=0.0186, k=31200, f_0=1.51 Hz and b=2.95). The wave-passage effect resulting from the difference in the arrival times of waves at support points is defined as Der Kiureghian (1996),

$$\left(\theta_{lm}(\omega)\right)^d = -\frac{\omega\, d_{lm}^L}{V_{app}} \quad (9)$$

where V_{app} is the apparent wave velocity and d_{lm}^L is the projection of d_{lm} on the ground surface along the direction of propagation of seismic waves. The apparent wave velocities employed in this study are $V_{app} = 200\,m/s$ for soft soil, $V_{app} = 600\,m/s$ for medium soil and $V_{app} = 1000\,m/s$ for firm soil. The site-response effect resulting from the differences in local soil conditions at the support points is obtained as (Der Kiureghian 1996),

$$\theta_{lm}(\omega)^z = \tan^{-1}\frac{Im\left[H_l(\omega)\,H_m(-\omega)\right]}{Re\left[H_l(\omega)\,H_m(-\omega)\right]} \quad (10)$$

where $H_l(\omega)$ is the local soil frequency response function representing the filtration through soil layers. For the soil frequency response function a model which idealizes the soil layer as a single degree of freedom oscillator of frequency ω_l and damping ratio ξ_l is used as shown below

$$\left|H_l(\omega)\right|^2 = \frac{\omega_l^2 + 2i\,\xi_l\,\omega_l\,\omega}{\omega_l^2 - \omega^2 + 2i\,\xi_l\,\omega_l\,\omega} \quad (11)$$

$$\left|H_m(\omega)\right|^2 = \frac{\omega^4}{\left(\omega_m^2-\omega^2\right)^2 + 4\xi_m^2\,\omega_m^2\,\omega^2} \quad (12)$$

where ω_l and ξ_l are the resonant frequency and damping ratio of the first filters, ω_m and ξ_m are the resonant frequency and damping ratio of the second filters, respectively. The auto-power spectral density function of the ground acceleration characterizing the earthquake process is assumed to be of the following form modified by Clough and Penzien (1983).

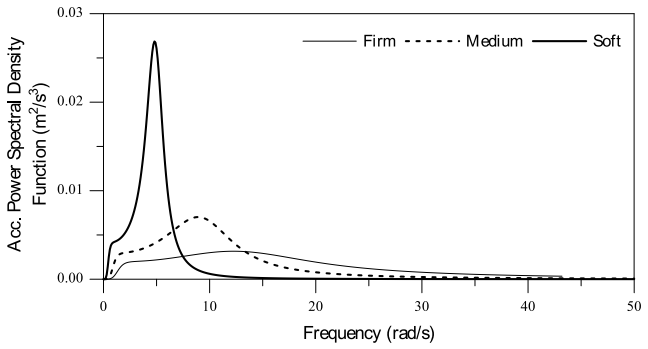

Fig. 1 Acceleration power spectral density functions for filtered white noise model of the DZC270 component record of 1999 Kocaeli Earthquake in Turkey

Table 1 The filter parameters for different soil types

Soil Type	ω_l (rad/sn)	ξ_l	ω_m (rad/sn)	ξ_m
Firm	15.0	0.6	1.5	0.6
Medium	10.0	0.4	1.0	0.6
Soft	5.0	0.2	0.5	0.6

Table 2 Properties of the deck and the towers of the cable-stayed bridge

Part of Structure	Cross-sectional Area (m^2)	Moment of Inertia I_x (m^4)	Moment of Inertia I_z (m^4)	Young's Modulus (kN/m^2)	Shear Modulus (kN/m^2)	Weight per unit length (kN/m)
Deck	0.827	19.76	0.34	210 000 000	80 769 230	118.59
Tower Part 1	14.120	28.06	532.20	30 787 000	12 351 200	339.30
Tower Part 2	14.120	27.80	795.20	30 787 000	12 351 200	339.30
Tower Part 3	30.750	30.71	1250.36	30 787 000	12 351 200	738.92

$$S_{\ddot{v}_g}(\omega) = S_o\left|H_l(\omega)\right|^2\left|H_m(\omega)\right|^2 \quad (13)$$

where S_o is the amplitude of the white-noise bedrock acceleration. In this study, firm (F), medium (M) and soft (S) soil types proposed by Der Kiureghian and Neuenhofer (1991) are used. The filter parameters for these soil types are utilized as presented in Table 1. The amplitude of the white-noise bedrock acceleration (S_o) is obtained for each soil type by equating the variance of the ground acceleration to the variance of the DZC270 Duzce component of 1999 Kocaeli Earthquake in Turkey. The calculated values of the intensity parameter for firm, medium and soft soil types are $S_o = 0.021338\,m^2/s^3$, $S_o = 0.031707\,m^2/s^3$ and $S_o = 0.044515\,m^2/s^3$ respectively. Acceleration power spectral density function for each soil type is presented in Fig. 1.

3. Application

In this study Quincy Bay-view Bridge crossing the Mississippi River at Quincy, Illinois, USA is selected as an example. The bridge consists of two H-shaped concrete towers, double-plane fan type cables, and a composite concrete-steel girder bridge deck. The main span is 274 m and there are two equal side spans of 134 m for a total

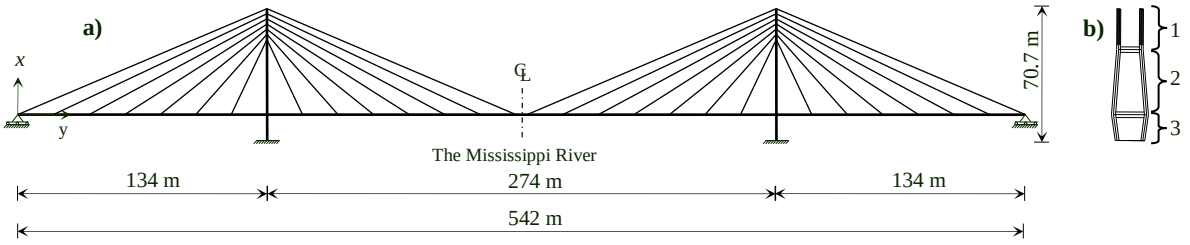

Fig. 2(a) Two dimensional Quincy Bay-view Bridge model, (b) cross-section of the tower

Table 3 Properties for the stay cables of the cable-stayed bridge

Cable Number	Cross-sectional Area (m^2)	Cable Weight (kN/m)	Young's Modulus (kN/m^2)
1	0.0180	1.76580	210 000 000
2	0.0135	1.32435	210 000 000
3	0.0107	1.04967	210 000 000
4	0.0070	0.68670	210 000 000

length of 542 m. The heights of the towers are 70.71 m from the waterline. There are a total of 56 cables, 28 supporting the main span and 14 supporting each side span. The cable members are spaced at 2.75 at the upper part of the towers and equally spaced at the deck level on the side as well as main spans (Fig. 2). The width of the deck from center to center of cables is 12 m.

The bridge tower consists of two concrete legs. There are three changes in the leg cross-section over the height of the towers. The bridge deck is assumed to be a continuous beam rigidly connected to the towers such that the deck moment will not be transferred to the tower through the deck-tower connection. The relevant properties of the bridge deck and towers are given in Table 2, while those of the cables are given in Table 3.

The finite element model of the cable-stayed bridge is constituted in SVEM software (Dumanoğlu and Soyluk, 2002). This software can be used for stochastic dynamic analyses of engineering structures considering spatially varying ground motions. Two-dimensional finite element model of the Bridge with 87 nodal points, 84 beam elements and 28 truss elements is considered for the analysis. The selected finite element model of the bridge is represented by 255 degrees of freedom. While the deck and towers are represented by beam elements, the cables are represented by linear elastic truss elements. The stiffness characteristics of an inclined cable can exhibit a nonlinear behavior caused by cable sag. This nonlinear behavior can be taken into account by linearization of the cable stiffness using an equivalent modulus of elasticity that is less than the basis material modulus (Ernst 1965). For the analysis of the bridge under consideration, Wilson and Gravelle (1991) found the value of equivalent modulus essentially equal to the true modulus of elasticity.

The response of a structure to spatially varying seismic excitation is greatly influenced by the relationship between ground wave speed, distance between supports and natural frequencies, its mode shapes and the direction of the excitation. To put it another word, the seismic response of structure depends on the frequency of seismic motion. The variation of fundamental period certainly effects the seismic

Table 4 Natural frequencies, fundamental periods of the bridge

Mode No	Frequency	Period
1	0.47482	2.10604
2	0.65622	1.52389
3	0.99664	1.00337
4	1.09063	0.91690
5	1.31190	0.76225
6	1.61124	0.62064
7	1.66880	0.59923
8	1.74225	0.57397
9	2.09363	0.47764
10	2.19949	0.45465
11	2.48503	0.40241
12	2.66937	0.37462
13	2.75877	0.36248
14	2.91979	0.34249
15	3.46224	0.28883

response of the bridge. Each mode will have "resonant wave speeds" which give rise to peaks and troughs in the modal response. Therefore, the response of the different modes provide a means of interpreting the global results and can be found by plotting the modal zeroth spectral moments (mean square response) against time delay. The modal responses of the cable-stayed bridge, such as the natural frequencies and mode shapes are given in Table 4.

In the Table, the first column presents the mode number of the bridge, the second and third columns present their natural frequencies (f) and fundamental periods, respectively. Beside, the first 15 modes for the bridge model are displayed in the relevant Table. The first two modes of the bridge are transverse, the next two modes are vertical, and the fifty mode is torsional mode. The Table shows the fundamental mode of the bridge at a frequency of 0.47482 Hz (period of 2.10604 sec) and the frequency of the bridge range from 0.47482 Hz to 3.46224 Hz for the first 15 modes.

In this paper, stochastic analysis of the cable-stayed bridge subjected to spatially varying ground motions by taking into account the incoherence, wave-passage and site-response effects is performed for variable local soil cases. For this purpose, the following three different soil condition cases are considered for the bridge supports. The spatially varying ground motion is applied to bridge supports in

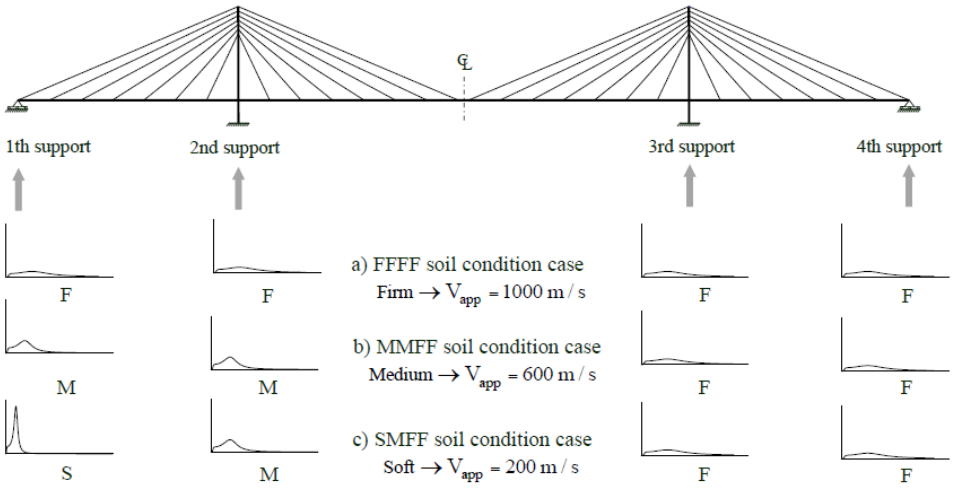

Fig. 3 The bridge subjected to spatially varying ground motions in the vertical direction for the various soil condition cases

vertical direction. The bridge subjected to spatially varying ground motions for the various soil condition cases and the various apparent wave velocities are shown Fig. 3. In the first soil case, all the supports are assumed to be founded on soils with firm soil type (FFFF). In the second soil case, while the first two supports of the bridge are assumed to be founded on medium soil, the remaining supports are assumed to be founded on firm soil type (MMFF). In the last soil case, the first and second supports of the bridge is founded on respectively, soft and medium soils, the remaining supports are founded on firm soil (SMFF).

The analysis is obtained for 2% damping ratio and for the first 15 modes. The stiffening effects of the cables caused by the dead load are also accounted for in the analysis. The filtered white noise ground motion model modified by Clough and Penzien (1993) is used and applied in the vertical direction as a ground motion model where the spectral density function intensity parameter is determined according to DZC270 component of the Duzce record of the Kocaeli Earthquake in 1999. The filtered white noise ground motion model is widely used to stochastic analyses for facilitate the conducted analyses by convert the time domain data and graphics to frequency domain.

4. Numerical results

Variance of total response has three components; the pseudo-static, the dynamic and the covariance components between the pseudo-static and dynamic components. Contribution of the each component to the total responses of the bridge is examined in this part. The process of normalisation is carried out by dividing the variance values by the maximum total response. The relative contribution of each component to the total vertical displacement along the bridge deck for FFFF, MMFF and SMFF soil condition sets are depicted in Fig. 4. As can be observed, the total displacements are dominated by the dynamic component for different soil conditions. However, the contribution of the dynamic component to the total response decreases and the contribution of the pseudo-static component increases while

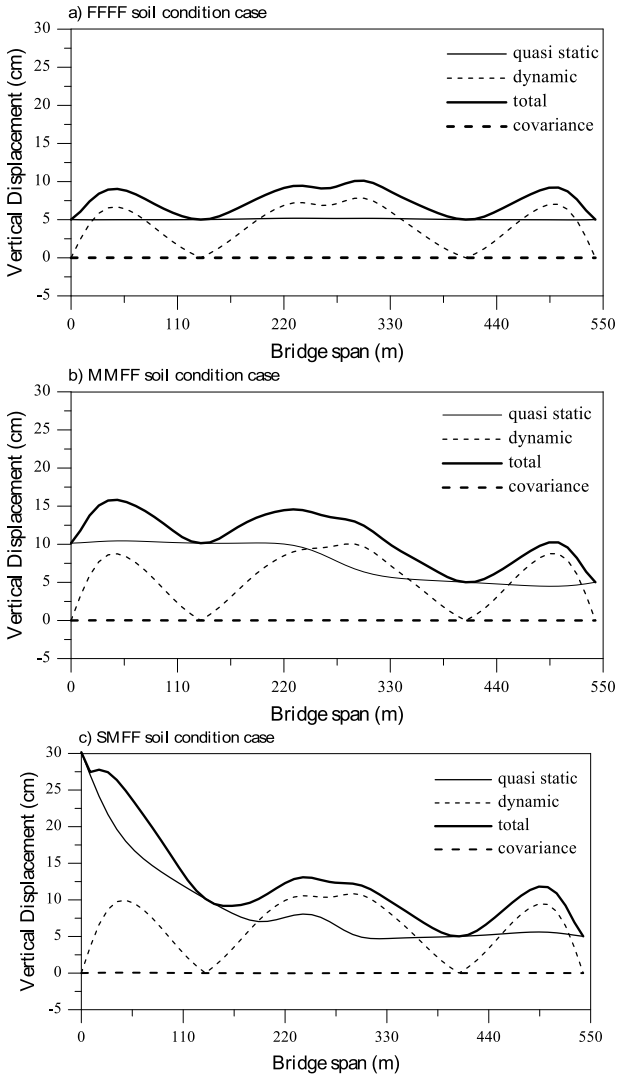

Fig. 4 Normalised displacement variances of the deck for various soil condition cases

the soil condition changes from hard to soft. Furthermore, for FFFF soil condition case, the bridge supports are assumed to be the same, displacements of dynamic and

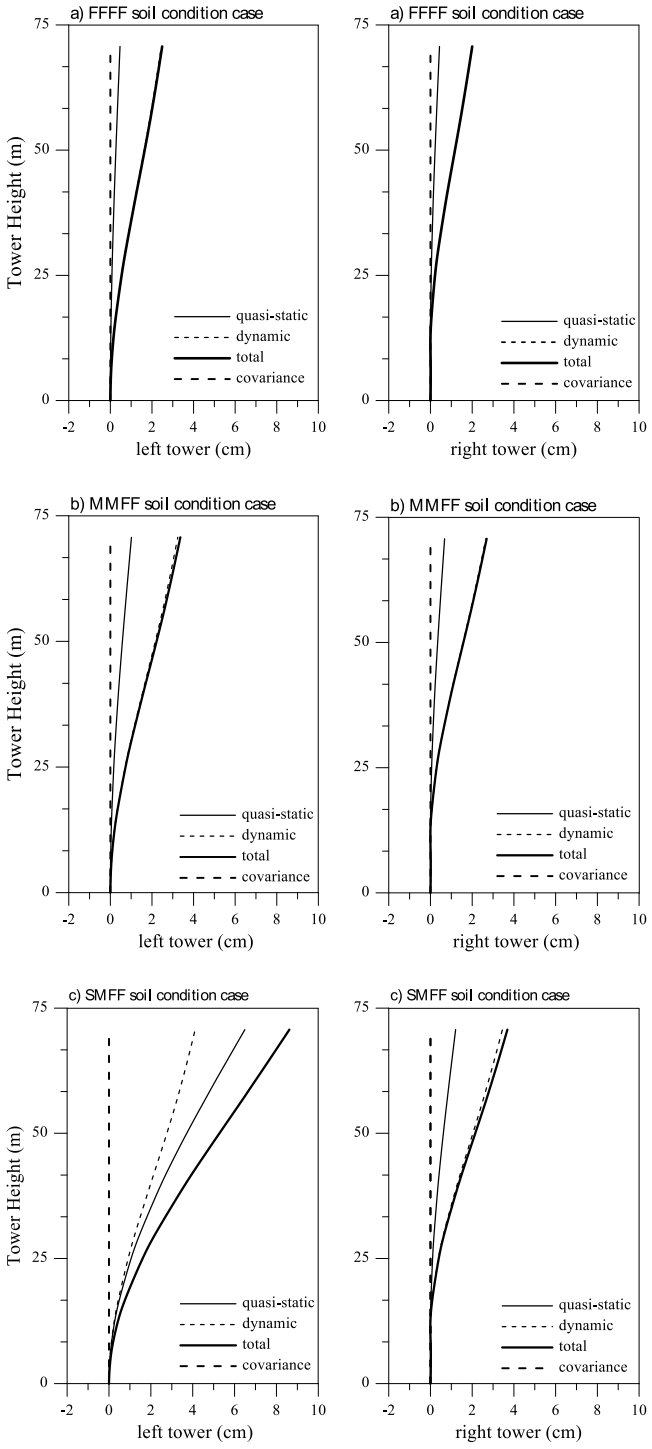

Fig. 5 Normalised displacement variances of left and right towers for various soil condition cases

pseudo-static components are almost symmetrical according to the middle of the bridge span. However, these displacements rather change and are not symmetrical any more as soil conditions of the supports along the deck chances from firm to soft. While the maximum vertical displacement of total component is nearly 10 cm for FFFF soil case, that displacement is nearly 30 cm in the first support of the bridge for SMFF soil case.

The relative contribution of the response components to the total horizontal tower displacements at the left and right

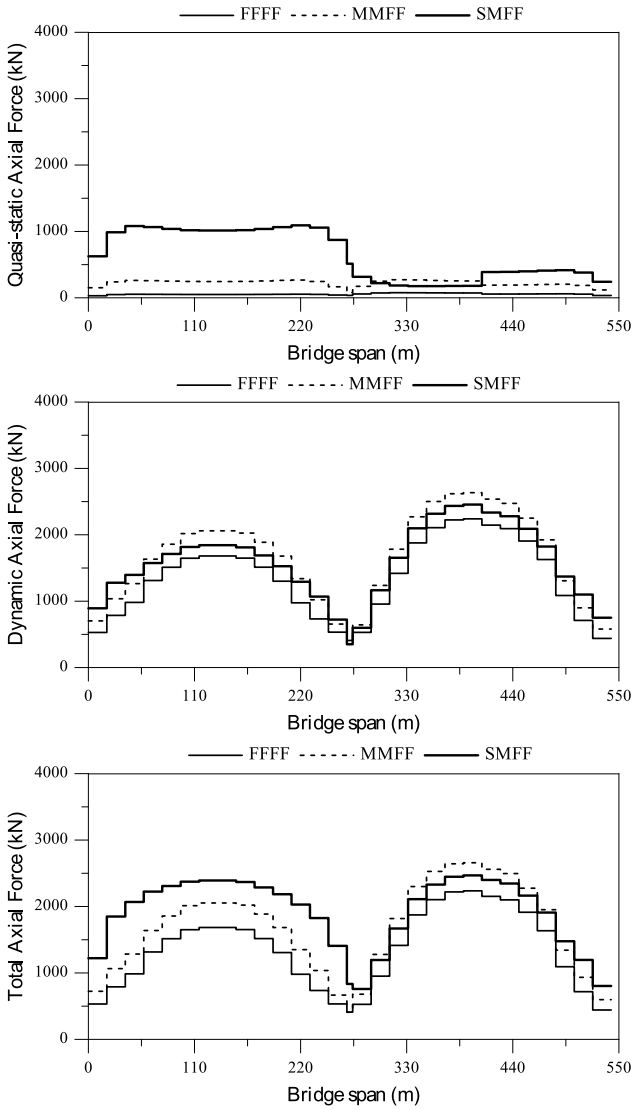

Fig. 6 Mean of maximum axial forces of the deck for different soil condition cases

towers is shown in Fig. 5 for different soil conditions. As can be seen, the variations obtained for the displacements at the right tower are similar for each soil condition case, while the variations obtained for the left tower are somehow different. At the left tower top point where maximum total horizontal displacement occurs, it can be observed that the pseudo-static component contributes 18.6, 30.1, 75.3 % and the dynamic component contributes 98.3, 96.3, 47.8 % for FFFF, MMFF, SMFF soil condition cases, respectively. Similarly, at the right side tower top point the pseudo-static component contributes 21.0, 25.0, 32.0 % and the dynamic component contribute 100.0, 98.0, 93.0 % for FFFF, MMFF, SMFF soil condition cases, respectively. At the both towers top point, the covariance component to maximum total horizontal displacement is nearly close to zero for all soil condition cases. At the left tower contribution of the dynamic component to the total displacements is more effective for FFFF and MMFF soil condition cases, while contribution of the pseudo-static component is more distinct for SMFF soil condition case.

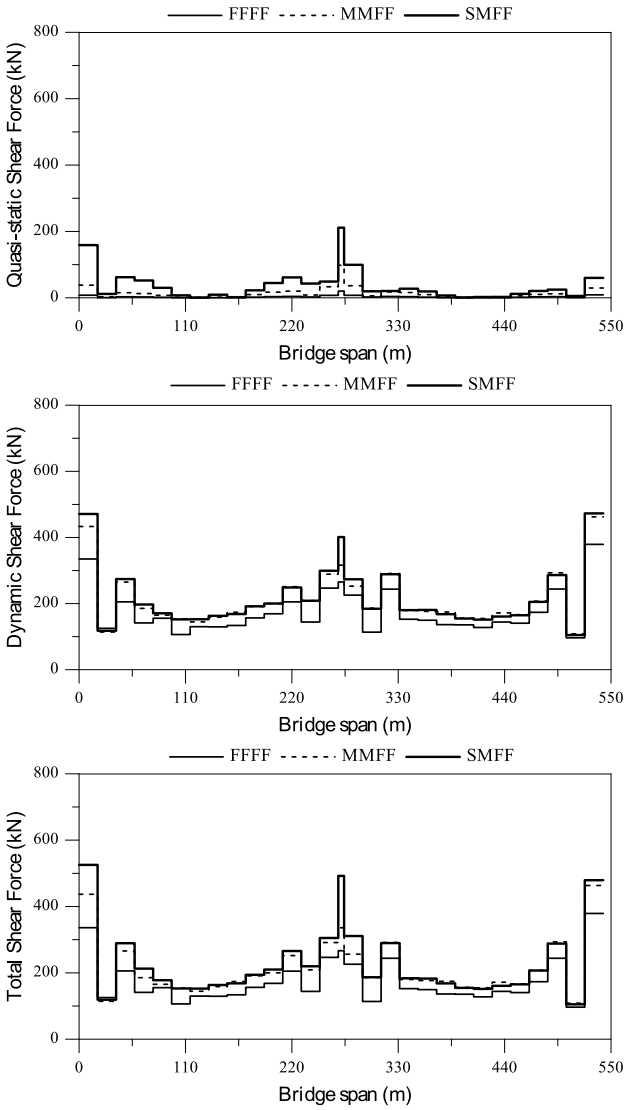

Fig. 7 Mean of maximum axial forces of the deck for different soil condition cases

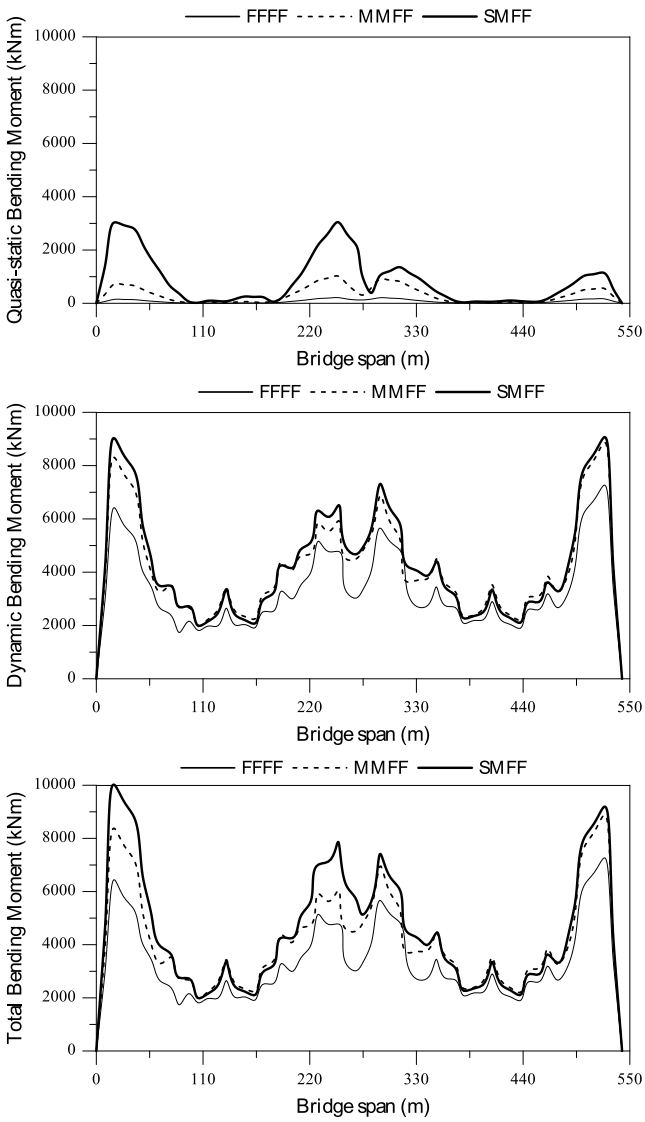

Fig. 8 Mean of maximum bending moments of the deck for different soil condition cases

The reason is that the left tower support soil conditions range from firm to soft and that amplify the pseudo-static components. At the right tower, the dynamic components largely dominate to the total responses for each soil condition case. The contribution of the pseudo-static component to the total displacement increase as bridge support soil conditions changes from firm to soft and that is more apparent for SMFF soil condition case.

Mean of maximum axial force responses for the deck is examined for the previously defined soil condition cases identified as FFFF, MMFF and SMFF. Mean of maximum pseudo-static, dynamic and total axial forces along the deck is depicted for various soil condition cases in Fig. 6. As can be seen from the figure that the axial forces generally increase as the bridge support soil conditions changes from FFFF to SMFF. The axial forces are maximum at the deck–tower junction points and are minimum at the anchorage support points and in the middle span of the deck. It can be obtained that maximum pseudo-static axial forces are 77.1 kN, 272.3 kN and 1091.9 kN, whereas maximum dynamic axial forces are 2240.5, 2634.8 and 2455.6 for FFFF, MMFF and SMFF soil condition cases, respectively. It is obtained that when the bridge supports located on SMFF soil condition case, maximum dynamic and pseudo-static axial forces, respectively, becomes 10% and 1400% larger than for FFFF soil condition case.

In Fig. 7, mean of maximum pseudo-static, dynamic and total shear forces is depicted for different soil condition cases identified as FFFF, MMFF and SMFF. As can be seen from the figure that the shear forces generally increase along the deck as the bridge support soil conditions changes from hard to soft. The shear forces are maximum at the anchorage support points and in the middle span of the deck and are minimum at the deck–tower junction points. It can be obtained that maximum pseudo-static shear forces are 20.3 kN, 98.1 kN and 211.3 kN, while maximum dynamic shear forces are 379.1 kN, 462.3 kN and 472.8 kN for FFFF, MMFF and SMFF soil condition cases, respectively. It is apparent that when the bridge supports located on SMFF soil condition case, maximum pseudo-static and

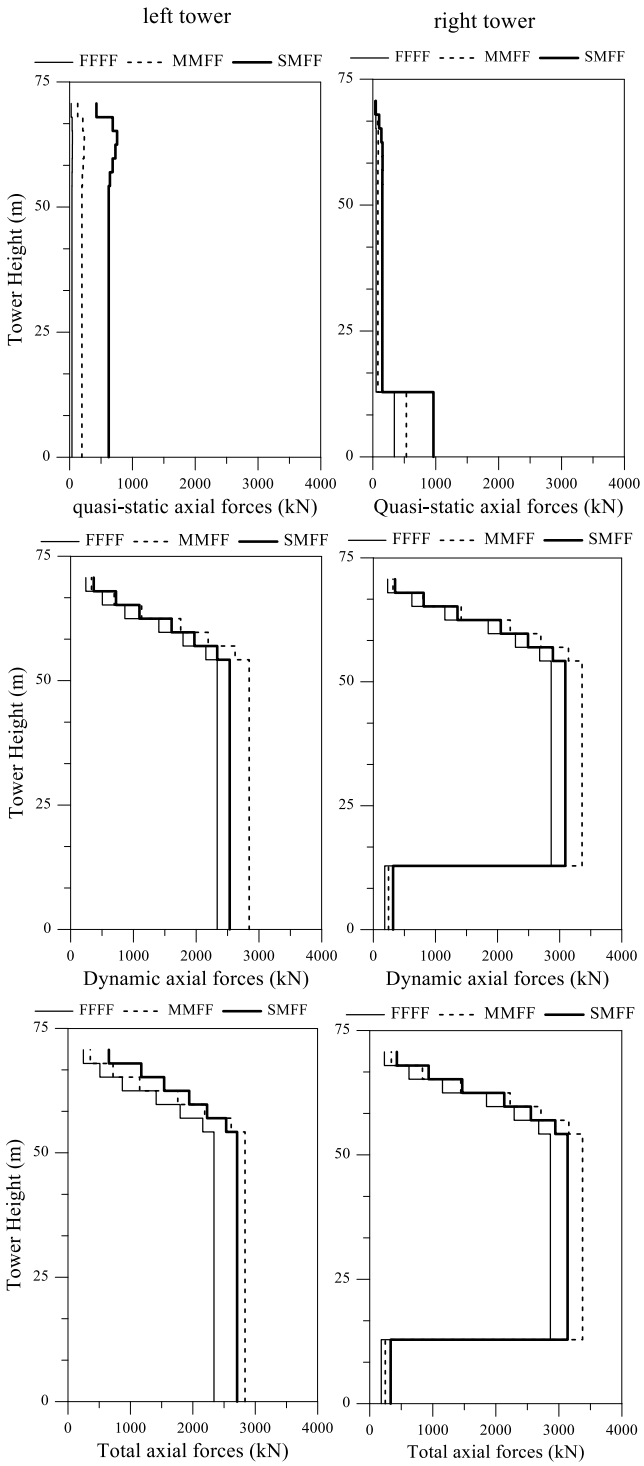

Fig. 9 Mean of maximum axial forces of the towers for different soil condition cases

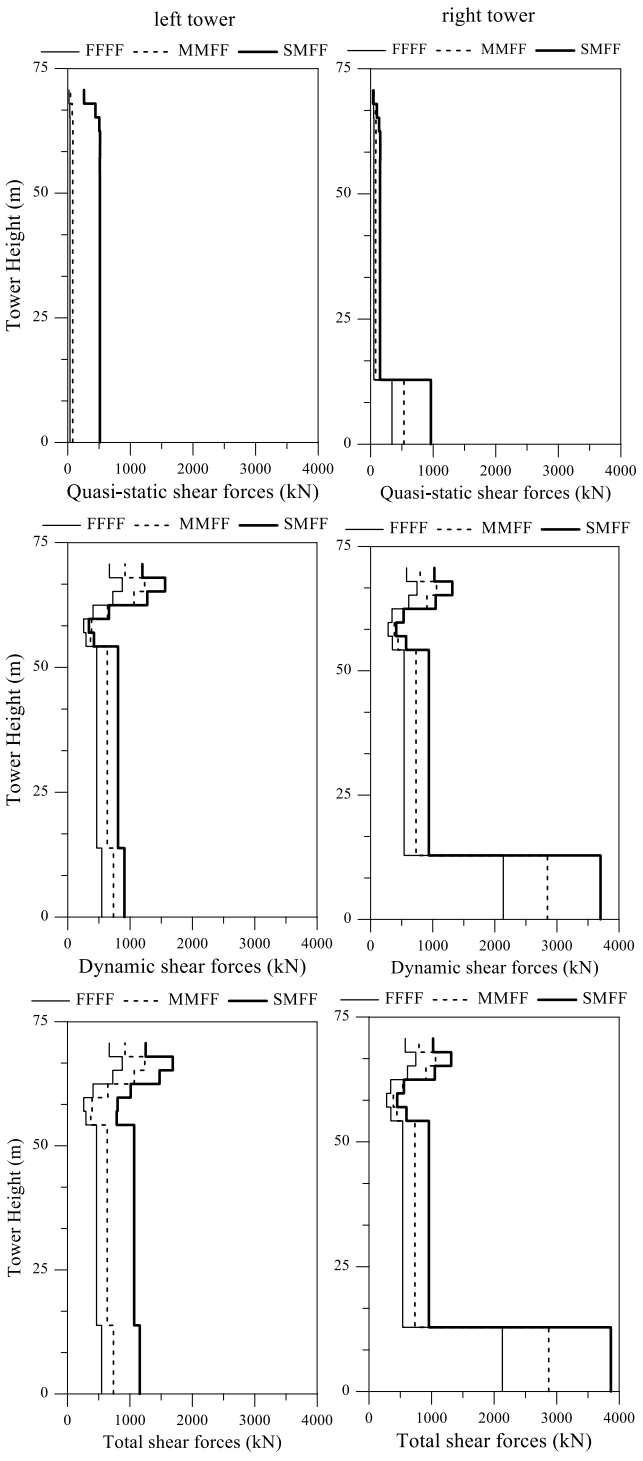

Fig. 10 Mean of maximum shear forces of towers for different soil condition cases

dynamic axial forces, respectively, are larger than ten times and 24% in accordance with FFFF soil condition case.

Mean of maximum pseudo-static, dynamic and total bending moments is indicated for different soil condition cases in Fig. 8. It can be seen that bending moments of the deck increase as the bridge support soil conditions changes from firm to soft. It is apparent that maximum bending moments take place either at points close to the abutments or at the close to the middle span of the bridge for all soil condition case. The obtained maximum pseudo-static bending moments are 213.6 kNm, 1024.9 kNm and 3048 kNm, while maximum dynamic bending moments are 7256 kNm, 8848.3 kNm and 9048.9 kNm for FFFF, MMFF and SMFF soil condition cases, respectively. The obtained bending moments increase as the bridge support soil conditions change from FFFFF to SMFF.

Mean of maximum pseudo-static, dynamic and total axial forces of the left and right towers depicted for various

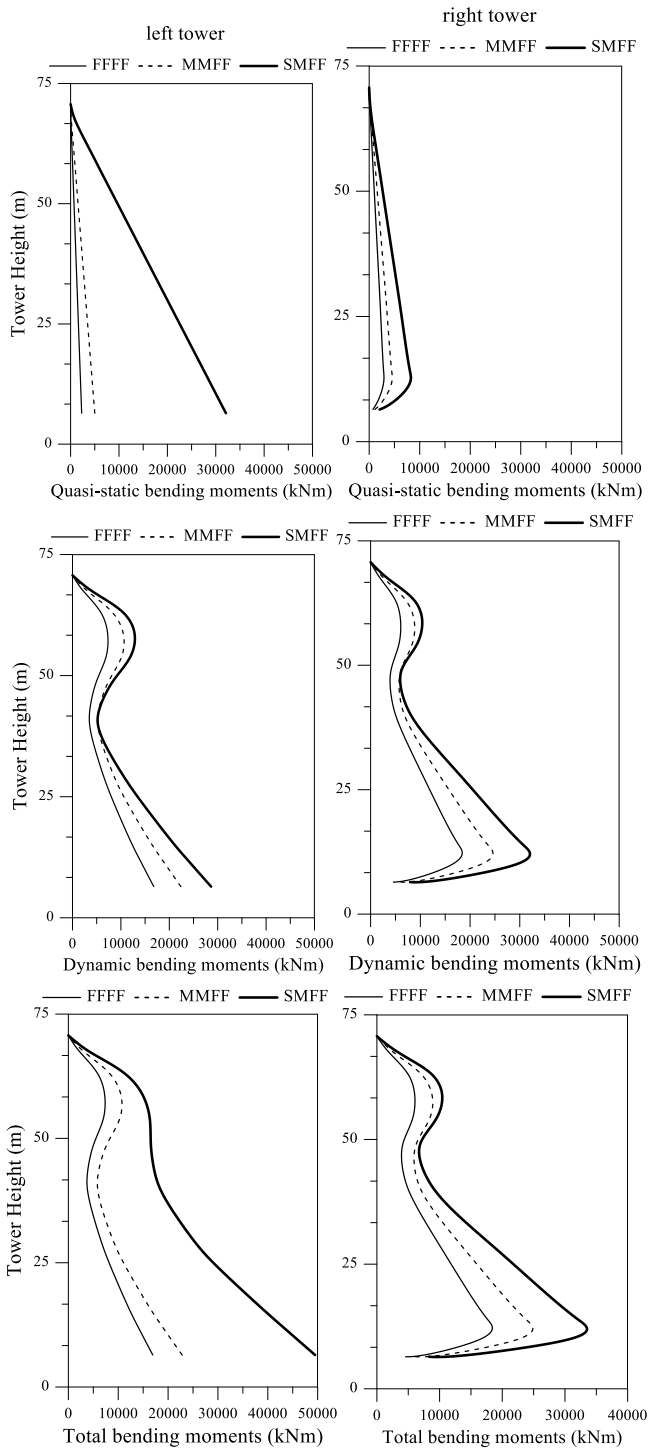

Fig. 11 Mean of maximum bending moments of towers for different soil condition cases

soil condition cases identified as before in Fig. 9. It is apparent that the pseudo-static axial forces are maximum for SMFF soil condition case, whereas the dynamic and total axial forces are generally maximum for MMFF soil condition case. Besides, the dynamic axial forces are much larger values in accordance with quasi-static axial forces for all soil condition case. As the Figure is also seen, axial forces of left and right towers are not the same, and the dynamic axial forces consisted of in both towers are much larger than pseudo-static axial forces for all soil condition case. In the Right tower, maximum dynamic and total axial forces consist of in the second part of the tower. However, in the Left tower maximum dynamic and total axial forces are the same in the first and second part of the tower. It can be also seen that axial forces have the smallest values at the top of the tower for all soil condition cases.

Mean of maximum pseudo-static, dynamic and total shear forces of both towers of the bridge is described in Fig. 10. It can be seen that shear forces of Left and Right towers are not the same, and these forces are the largest for SMFF soil condition case in accordance with the other soil condition cases for both of the towers. The pseudo-static shear forces don't change much along the height of the tower and maximum of these forces are 37.6 kN, 82.4 kN and 516.1 kN in the Left tower, while these are 341.7 kN, 532.7 kN and 963.5 kN in the Right tower for FFFF, MMFF and SMFF soil condition cases, respectively. In the Left tower, maximum of these forces consist of in the third part of the tower where is close to the top of the tower. However, in the Right tower these forces occur in the first part of the tower where is close to the bottom of the tower.

Mean of maximum pseudo-static, dynamic and total bending moments of both towers of the bridge is described for various soil condition cases in Fig. 11. It is apparent that bending moments of left and right towers are not the same, and these forces are zero at the top of the towers. These forces are maximum at the bottom of the left tower, whereas these are maximum at the right tower in the close to the deck–tower junction points for all soil condition case. The changing of pseudo-static bending moments is nearly linear for the left tower, while it is not for the right tower. The obtained bending moments increases as bridge support soil conditions changes from hard to soft for both of the towers. The obtained maximum pseudo-static bending moments are 2287.8 kNm, 4996.9 kNm and 32102.9 kNm for the left tower and are 29301 kNm, 45676 kNm and 8261.2 kNm for the right tower. The obtained maximum dynamic bending moments are 16800 kNm, 22402.1 kNm and 28641.6 kNm for the left tower and are 18317 kNm, 24409.5 kNm and 31739.7 kNm for the right tower for FFFF, MMFF and SMFF soil condition cases, respectively.

5. Conclusions

In this study, it is intended to investigate the dynamic performance of a cable-stayed bridge model for variable local soil condition cases under the spatially varying ground motions. The main results from the study can be drawn as below:

• The obtained responses for varying soil condition cases give rise to larger responses than those of the same soil condition case. Therefore, the more difference between local soil condition cases of the bridge support, the more responses take place.

• When the all supports of the bridge are assumed to be founded on soils with hard soil type the variance values are dominated by the dynamic component. On the other hand, at the both of towers and the deck, the total displacements

are dominated by the dynamic component for the constant soil condition case where the bridge supports are the same, whereas the pseudo-static component dominates the total displacements for the varying soil condition cases where the bridge supports are different. Moreover, the relative contribution of the pseudo-static component to the total response mostly increases by varying between the local soil conditions from firm to soft.

• It is apparent that the total responses will give rise to larger responses for varying wave velocity cases compared to those of the constantly travelling wave velocity case, and what's more, the variation of the wave velocity has significant influence on the deck and both of towers total responses as compared with those of the constantly travelling wave velocity case. The difference of the wave velocities based on the properties of the local soil conditions where the bridge supports are erected has important influences on the dynamic behavior of the bridge. In addition, the variability of the ground motions should be considered in the analysis of long span cable-stayed bridges to obtain more accurate in calculating the bridge responses.

References

Adanur, S., Altunisik, A.C., Basaga, H.B., Soyluk, K. and Dumanoglu, A.A. (2017), "Wave-passage effect on the seismic response of suspension bridges considering local soil conditions", *Int. J. Steel Struct.*, **17**(2), 501-513.

Allam, A.M. (2010), "Multiple-support excitations of open-plane frames by a filtered white-noise and soil-structure interaction", *J. Sound Vibr.*, **329**(20), 4212-4226.

Allam, S.M. and Datta, T.K. (1999), "Seismic behavior of cable stayed bridges under multi-component random ground motion", *Eng. Struct.*, **21**(1), 62-74.

Ates, S., Dumanoglu, A.A. and Alemdar, B. (2005), "Stochastic response of seismically isolated highway bridges with friction pendulum systems to spatially varying earthquake ground motions", *Eng. Struct.*, **27**(13), 1843-1858.

Ates, S., Tonyali, Z., Soyluk, K. and Samberou, A.M.S. (2018), "Effectiveness of soil-structure interaction and dynamic characteristics on cable-stayed bridges subjected to multiple support excitation", *Int. J. Steel Struct.*, **18**(2), 554-568

Bai, C., Ma, H. and Shim, V.P.W. (2015), "Stochastic elastic wave analysis of angled beams", S*truct. Eng. Mech.*, **56**(5), 767-785.

Betti, R., Abdel-Ghaffar, A.M. and Niazy, A.S. (1993), "Kinematic soil-structure interaction for long-span cable-supported bridges", *Earthq. Eng. Struct. Dyn.*, **22**(5), 415-430.

Clough, R.W. and Penzien, J. (1993), *Dynamics of Structures*, 2nd Edition, McGraw Hill, Inc., Singapore

Der Kiureghian, A. and Neuenhofer, A. (1991), *A Response Spectrum Method for Multiple-Support Seismic Excitations*, Report No. UCB/EERC-91/08, Earthquake Engineering Research Center, College of Engineering, University of California, Berkeley, California, U.S.A.

Dumanoglu, A.A. and Soyluk, K., (2002), *SVEM, A Stochastic Structural Analysis Program for Spatially Varying Earthquake Motions*, TDV/KT 023-76, Turkish Earthquake Foundation, Istanbul, Turkey.

Ernst, H.J. (1965), "Der e-modul von seilen unter berucksiehtigung des durchanges", *Der Bauingenieur*, **40**(2), 52-75.

Garevski, M., Dumanoglu, A.A. and Severn, R.T. (1988), "Dynamic characteristics and seismic behavior of Jindo bridge, South Korea", *Struct. Eng. Rev.*, **1**, 141-149.

Geng, F., Ding, Y., Xie, H., Song, J. and Li, W. (2014), "Influence of structural system measures on the dynamic characteristics of a multi-span cable-stayed bridge", *Struct. Eng. Mech.*, **52**(1), 51-73.

Harichandran, R.S. and Vanmarcke, E.H., (1986), "Stochastic variation of earthquake ground motion in space and time", *J. Eng. Mech.*, **112**(2), 154-174.

Kim, S. and Kang, Y.J. (2016), "Structural behavior of cable-stayed bridges after cable failure", *Struct. Eng. Mech.*, **59**(6), 1095-1120.

Kuyumcu, Z. and Ates, S. (2012), "Soil-structure-foundation effects on stochastic response analysis of cable-stayed bridges", *Struct. Eng. Mech.*, **43**(5), 637-655.

Nazmy, A.S. and Abdel-Ghaffar, A.M. (1987), *Seismic Response Analysis of Cable Stayed Bridges Subjected to Uniform and Multiple-Support Excitations*, Report No. 87-SM-1, Department of Civil Engineering, Princeton University, Princeton, New Jersey, U.S.A.

Nazmy, A.S. and Abdel-Ghaffar, A.M. (1990), "Non-linear earthquake-response analysis of long-span cable-stayed bridges: Applications", *Earthq. Eng. Struct. Dyn.*, **19**(1), 63-76.

Nazmy, A.S. and Abdel-Ghaffar, A.M. (1992), "Effects of ground motion spatial variability on the response of cable-stayed bridges", *Earthq. Eng. Struct. Dyn.*, **21**(1), 1-20.

Soyluk, K. and Dumanoglu, A.A. (2000), "Comparison of asynchronous and stochastic dynamic response of a cable-stayed bridge", *Eng. Struct.*, **22**(5), 435-445.

Soyluk, K. and Dumanoglu, A.A. (2004), "Spatial variability effects of ground motions on cable-stayed bridges", *Soil Dyn. Earthq. Eng.*, **24**(3), 241-250.

Soyluk, K. and Yucel, K. (2007), "Verification of the filtered white noise model in the random vibration analysis of steel arch bridges", *J. Facult. Eng. Architectu. Gazi Univ.*, **22**(4), 933-939.

Thomas, E.P. and Marc, O.E. (1998), "Effects of spatially varying ground motions on short bridges", *J. Struct. Eng.*, **124**(8), 948-955.

Wang, D., Li, Y., Hao, S. and Zhao, D. (2016), "Wave-passage effect of earthquake loadings on long structures", *Int. J. Struct. Stabil. Dyn.*, **16**(7), 1550037.

Wang, J., Carr, A.J., Cooke, N. and Moss, P.J. (2009), "The response of a 344 m long bridge to non-uniform earthquake ground motions", *Eng. Struct.*, **31**(11), 2554-2567.

Wilson, J.C. and Gravelle, W. (1991), "Modeling of a cable-stayed bridge for dynamic analysis", *Earthq. Eng. Struct. Dyn.*, **20**(8), 707-721.

Yan, X., Xinzhi, D. and Jianzhong, L. (2014), "Seismic design strategy of cable stayed bridges subjected to strong ground motions", *Struct. Eng. Mech.*, **51**(6), 909-922.

Zhang, X.J. and Yu, Z.J. (2015), "Study of seismic performance of cable-stayed-suspension hybrid bridges", *Struct. Eng. Mech.*, **55**(6), 1203-1221.

Zhang, Y.H., Li, Q.S., Lin, J.H. and Williams, F.W. (2009), "Random vibration analysis of long-span structures subjected to spatially varying ground motions", *Soil Dyn. Earthq. Eng.*, **29**(4), 620-629.

CC